Analysis of Load Test on Composite I-Girder Bridge

F.Huseynov[1, 2], J.M.W. Brownjohn[3], E.J. O'Brien[2], D. Hester[4]

[1] Full Scale Dynamics LTD, Kay Building North Park Road, Exeter EX4 4QF
[2] School of Civil Engineering, University College Dublin, Richview Newstead Block B, Belfield, Dublin, Ireland
[3] Vibration Engineering Section, College of Engineering, Mathematics and Physical Sciences, University of Exeter, North Park Road, EX4 4QF Exeter, UK
[4] School of Natural and Built Environment, Queen's University Belfast, Stranmillis Road, BT9 5AG Belfast, Northern Ireland, UK

Contact author: Farhad Huseynov
Kay Building North Park Road,
Exeter. UK
EX4 6BH
E-mail: f.huseynov@fullscaledynamics.com
Tel: +447533118686

Body text word count: 4432
Number of figures: 10
Number of tables: 4

Abstract

This paper showcases the importance of field testing in efforts to deal with the deteriorating infrastructure. It shows that when tested, bridges do not necessarily behave as expected under load, particularly with respect to boundary conditions. This is demonstrated via a load test performed on a healthy but aging composite reinforced concrete bridge in Exeter, UK. The bridge girders were instrumented with strain transducers and static strains were recorded while a four-axle, 32 tonne lorry remained stationary in a single lane. Subsequently, a 3-D finite element model of the bridge was developed and calibrated based on the field test data. The bridge deck was originally designed as simply supported, however, it is shown (from the field test & calibrated model) that the support conditions were no longer behaving as pin-roller which affects the load distribution characteristics of the superstructure. Transverse load distribution factors (DFs) of the bridge deck structure were studied for different boundary conditions. The DFs obtained from analysis were compared with DFs provided in Design Manual for Roads and Bridges (DMRB) Standard Specification. Having observed in the load test that the ends of the deck appeared to be experiencing some rotational restraint, a parametric study was carried out to calculate mid-span bending moment (under DMRB assessment loading) for varying levels of restraint at the end of the deck.

Keywords:

Bridge Field Testing, Strain Measurements, Load Distribution Factors, FE Modelling, Bridge Assessment

1 Introduction

Bridges are expensive and critical structures that connect communities and serve as regional lifelines. Over time, they are exposed to many degradation processes due to environmental factors and changing loading conditions. It is found in recent studies that more than half of the Europe's 1 million bridges were built before 1965 and so they are nearing the end of their 50-year design lives [1]. Their replacement cost is equal to 30% of gross domestic product so it is not feasible to replace them. Thus, bridge owners are particularly interested in accurate and inexpensive methods for verifying remaining service life and safety of such aging structures.

Current bridge evaluation techniques are mainly based on qualitative assessment and can fail to estimate the hidden strength reserve of aging bridge assets in many cases. Based on such methods, more than 20% of 155,000 bridges in the UK are reported as structurally deficient in some form [2]. However, the actual load-carrying capacity of structures is often higher than predicted by analysis [3]. For example, a load test was performed on a decommissioned skewed I-girder steel bridge where test load of 17 times higher than the anticipated load was applied to the bridge and results showed that it had been decommissioned despite a significant remaining load capacity [4]. In another study, a 50-year-old Swedish reinforced concrete railway bridge was tested to failure [5]. The results indicated that the bridge could sustain almost five times the design load. Those reserve capacities come from additional sources of strength not normally taken into account in the conventional assessment methods and is associated to several factors such as higher girder/deck composite action, superior material strength, girder end restraints, dynamic impact, unexpected transverse load distribution due to material inelasticity, contribution of non-structural elements such as curbs, parapets and etc. Thus, field testing is an important topic in an effort to deal

with the deteriorating infrastructure, since it can reveal hidden reserves of structural strength at the same time verifying safety.

Current bridge evaluation specification in the UK, Design Manual for Roads and Bridges (DMRB), is built on already available design standards, which contain degrees of uncertainty that understandably lead to conservative results. Although they fit the purpose for the design of new structures, for the assessment of aging bridge assets such uncertainties add up and can obscure the remaining strength reserve of structures. One of the main sources of such uncertainties involved in DMRB Standard Specification is associated with the methods used for calculating the load effects for assessment purposes. For example, transverse load distribution factors (DFs) recommended by the code are typically quite high. Obviously the values given in the code have to cover a wide range of bridge types and loading conditions and as a result are understandably conservative. However, the reality is that every bridge presents a unique situation which has its own characteristics and requirements.

To demonstrate the kind of 'individual behaviour' that a bridge can have, i.e. different to the idealised behaviour expressed in the DMRB Standard Specification, this study presents the results of a load test performed on a composite reinforced concrete bridge in Exeter, UK where strain transducers were installed on bridge girder soffits and quasi-static strain response were recorded under 32 tonne, four axle truck loading. In parallel, a 3 – D FE model of the structure was developed and calibrated based on the load test data to study the behaviour of the structure under static loading. The bridge support conditions were originally designed to move freely in the longitudinal direction however, it was observed during the FE model calibration that the bridge boundary conditions no longer behave this way and the structure experiences a certain level of restraint at support locations. Load-shedding characteristics of the

superstructure were also studied within the scope of this work where DFs of the deck structure were calculated for different boundary conditions and compared with the DF value provided in DMRB Standard Specification for a similar bridge type. Having observed the change in the boundary conditions, a parametric study was conducted to study the effect of translational restraint on load effects under DMRB assessment loading. Load effects were calculated for varying levels of translational restraints at the end of the deck and it was demonstrated through parametric studies that an accurate representation of boundary conditions could reveal strength reserves in a bridge during a bridge assessment.

2 Test Structure

Two almost identical adjacent bridges known as Exe North and South Bridges form a large roundabout spanning the River Exe in Exeter, UK. Exe North Bridge was chosen as a test structure. It is 59.35m long and consists of two 19.85m outer spans and a 19.61m centre span, resting on two wall-type pier structures in the river and abutments at the ends. It was constructed in 1969 to replace the previous three-hinged steel arch bridge.

The superstructure is 18.9m wide, carrying four lanes of traffic and connecting Okehampton Street (South) with Bonhay Road (North). The first lane is 4m wide and designated as a bus lane. The other three lanes are 3 – 3.25m wide and used by public traffic. The superstructure is 1m deep and consists of 12 composite precast girders placed at 1.53m apart and a 0.23m deep cast in situ reinforced concrete deck. The girder elements were designed as composite type, where steel beams were embedded in reinforced concrete I-girders. The steel beams are 762x267x197 mm universal beams with additional plates welded to the top and bottom flanges. Full composite action between steel and concrete girders is provided through double shear connectors, closely placed (125mm) at supports and gradually increasing towards the mid-span (500mm).

The substructure consists of two wall-type pier structures and two cantilever type abutments at 15 degrees skew with respect to spans and parallel to the river bank. The connection between superstructure and substructure is provided with laminated elastomeric bearings which consist of alternating layers of rubber and steel plates and are designed to produce a vertically stiff but longitudinally flexible support conditions for bridge structures. Continuity between spans is cut off by 10 – 25mm wide gaps

filled with bituminous rubber so that each span is simply supported.

Fig. 1 (a), (b) and (c) respectively show the bridge elevation, plan and cross section. Fig. 2 shows a picture of the bridge, and the structural characteristics of the bridge summarized in Table 1. Since the spans are not continuous, only the north span was chosen for testing purposes (this is the right hand span in Fig. 2).

3 Instrumentation and Testing

ST350 model strain transducers provided by Bridge Diagnostics, Inc. (BDI) were used to measure the strains during the field test. These are reusable Wheatstone full bridge resistive sensors encased in rugged transducer packages that are mounted on the structure with bolted tabs. The strain sensor itself is 76mm long, but the gauge length of sensors is 0.6 m as aluminium extension rods are used to account for local microcracks that can occur in RC structures and average strain values are recorded. Fig. 3 shows the sensor installed on a girder soffit. These sensors are wired into three 4-channel nodes wirelessly linked to a host data acquisition system. The data are recorded with a sampling rate of 250 Hz. Based on the gain, excitation and full-scale range of the sensors and software settings, 0.3 microstrain resolution is determined for the measurement readings.

The bridge spans over water, which made installation a difficult task. The only access to the deck soffit, (avoiding working in water), was at the quarter span, through the 5 m wide footpath along the river bank. Hence, the strain transducers were installed on each girder soffit at quarter span close to the North abutment. Ideally, it would have been nice to also be able to record strains at midspan during the test as this would provide another set of measurements to check the numerical model against, unfortunately in this case this was not logistically possible. However, having multiple measurements (i.e. gauges installed at each girder) at the quarter span helped to calibrate the FE model as accurate as possible. Gauges installed on each girder also allow the load – shedding characteristics of the superstructure to be studied. The plan view of the sensor layout is provided in Fig. 4. The beams are indicated as red lines and the sensors are labelled 1-12.

The test vehicle used was a four-axle 32 tonne lorry, and this was used to obtain quasi-

static strain response. Fig. 5 (a) shows the truck during the load test. It has axle spacing of 1.94 m, 3.56 m and 1.35 m from front to rear. Fig. 5 (b) depicts the axle configurations and Table 2 tabulates weight for each axle. The truck made several passes in each of the four lanes (Lane 1, Lane 2, Lane 3, and Lane 4), stopping every time for 30-45 seconds to record the quasi-static strain. The front axle of the truck, while it was stationary, aligned approximately with the supports at the north abutment, with vehicle centre of gravity in line with sensor locations. Fig. 4 illustrates the positioning of the vehicle in each of the four lanes. 16 passes were made in total (4 passes per lane) and the test was performed overnight to avoid traffic on the bridge. In the load cases corresponding to Lane 1 and Lane 4, the exterior most wheel line is approximately 0.8 m and 0.3 m from the kerb, respectively.

Fig. 6 illustrates a typical strain-time history recorded during the test. Fig. 7 shows the average strain calculated in each girder for truck positions in Lane 1-4. The implications of the test are described in detail in the following sections.

4 Numerical Model of the Bridge

Since it was not possible to install the sensors at midspan of the deck structure, a 3-D FE model of the bridge was developed to study the load effects at midspan location under similar loading conditions applied during the field testing. The FE model was developed according to available structural design drawings using ANSYS V16.0 software [6]. The model includes all the necessary geometric details with composite structural configurations. The model was developed using SOLID185 elements to obtain reliable strains and accurate representation of steel concrete composite behaviour. Since the spans are non-continuous and independent, only the tested (North) span was considered during the modelling. Fig. 8 (a) illustrates the FE model of steel stringers and Fig. 8 (b) shows full/final 3-D FE model of the Exe North Bridge.

The bridge model represents concrete I-girders, steel stringers with stiffening plates at top and bottom flanges. Each part of the model was developed separately in ANSYS native scripting language, with parts merged using the NUMMRG command to form the complete model of the Exe North Bridge structure. Subsequently, mesh verification analysis was carried out where several mesh sizes were investigated until the midspan deflection is converged under an arbitrary load. Mesh size of 250 mm was eventually chosen. Designed mesh size was also sufficiently fine to be able to simulate different truck loading conditions over the bridge.

Pier and abutment structures were excluded from the FE model as they are assumed to be infinitely rigid in axial directions. At each support location, the elastomeric bearings were represented in the numerical model by releasing the longitudinal displacements. During the model calibration, different boundary conditions were considered and these are described in detail in the following section. Many previous

studies investigated the effect of skew angle on load distribution characteristics of bridge deck structures and it has been reported that skew has little effect (<1%) for an angle smaller than 20 degrees for this type of bridge [7, 8]. Therefore, the bridge was modelled without a skew angle.

5 Results and Discussions

Similar load cases applied during the load test were simulated on the 3-D FE model and different boundary conditions were studied to understand the behaviour of the structure under static loading. Strain values predicted for each boundary condition using numerical model were compared with data obtained from the field test. It was observed that the bridge boundary conditions have likely changed compared to the likely original design assumption, i.e. being simply supported (section 5.1). Later, the calibrated model was used to study the likely load-shedding characteristics of the bridge which were compared to those prescribed by the DMRB Standard Specification (section 5.2). Finally, a parametric study was carried out to examine how the load effects under assessment loading specified by DMRB Standard Specification are affected by changes to the boundary conditions (section 5.3).

5.1 Comparing FE strain predictions to field data

Once the average strain values for each girder were obtained based on the field test (Fig. 7), similar loading cases were simulated using the FE model. Fine meshing made it possible to locate accurately the truck axle configuration at each lane. Several scenarios were studied to understand the current structural condition of the bridge and its behaviour under applied load which are discussed in detail below.

Ultimately, three different boundary conditions were studied to investigate the behaviour of the bridge deck. However, initially, only two were simulated. In the first case, the bridge support conditions were assigned as a hinge at one end and roller at the other end (hinge-roller case), which is similar to the likely initial design assumption. In the second case, longitudinal movement of supports at both ends was restrained (hinge-hinge case). Fig. 9 (a)-(d) show the measured and theoretical girder

strains (for different boundary conditions) for the truck positioned in lanes 1-4 respectively. Results show that measured (test) strains (black plot, diamond data markers) lay between two limits of boundary conditions, hinge-hinge (red plot, star data markers) and hinge-roller (green plot, circular data markers), which implies that bridge boundary conditions are partially restrained. The third boundary condition tried to simulate this partial restraint by taking the hinge – roller model and adding longitudinal springs to the top and bottom flanges at the ends of the girder. Fig. 10 shows the schematic drawings of the three cases of boundary conditions used for finite element analysis. Having longitudinal spring at top and bottom flange of the girder for the partially restrained boundary condition is the equivalent to a rotational restraint. The springs were modelled with springs using ANSYS COMBIN14 elements attached to top and bottom flanges of girders. Springs at the bottom flanges represent the longitudinal stiffness of the elastomeric bearings whereas at top flanges they represent the longitudinal restraint provided by the expansion joint. Estimating the degree of partial stiffness of the elastomeric bearings was a challenging task. To have an idea about the maximum possible level of restrain, initially, equivalent spring coefficient that would reproduce the hinge – hinge boundary condition was predicted as ~24 MN/mm by trial and error method. Admittedly elastomeric bearings are not designed to have such a degree of longitudinal stiffness however, it guided as a known datum for obtaining the degree of longitudinal stiffness for partially restrained boundary condition. In reality, the degree of partial fixity also can vary from girder to girder and it is difficult to identify such differences accurately and apply the corresponding spring coefficients. In this study, girders were grouped, and suitable spring coefficients (K_{spr}) for partially restrained boundary condition were chosen by trial and error. The degree of longitudinal stiffness of elastomeric bearings varied between 1.2 – 2.4 MN/mm. It was concluded that movement of elastomeric bearings in the

longitudinal direction is partially fixed. It was also observed that bearings under girders 3-8 are more restrained than the others. This is not surprising as girders 3-5 correspond with the bus lane (Lane – 1) which is more heavily loaded than the others. Also, girders 6-8 are located at the centreline of the roadway which are exposed to more loads due to the typical load-shedding path between girders, which is described later in Fig. 11. Results obtained from the FE model with partially restrained boundary conditions (blue plot, triangular data markers) are in good agreement with the field test data for all 4 lanes. The foregoing study clearly shows that changes in bearing conditions, i.e. a degree of rotational restraint at the supports significantly reduce load effect (tensile stress in bottom fibre) in the bridge girder This restraint at the end of the deck could impact on the load carrying capacity of the bridge in a positive way, i.e. reducing the stress in the extreme fibre at mid-span. Admittedly this reduction in the expected stress in the bottom fibre at mid-span may have negative outcomes in other parts of the deck, i.e. increases in stress, so that needs to be taken into consideration. However, the above results demonstrate that field testing is an important tool when evaluating aging bridge assets as it could reveal hidden strength reserves which current bridge inspection techniques fail to identify.

5.2 Distribution factors

Transverse load distribution factors (DFs) are a measure of the transverse load transfer through the structure. Bridges are typically designed in such a way that traffic load is distributed between girders as "fairly" as possible so as not to overstress any particular load carrying member. Therefore, in load carrying assessment of a beam and slab bridge, the DFs specified by the code play a very important part in the calculation. For example, when a load is in a particular lane, a high DF implies there is little load sharing between adjacent girders and therefore the portion of the load carried by the

girder(s) under the load is assumed to be quite high and assessment will be conservative. Therefore, obtaining DFs is of vital importance for any bridge assessment activity.

Any change in bridge condition during its service life might significantly affect its load distribution characteristics. Having seen in the previous section how the magnitude of strain is affected by changes in the boundary conditions, in this section the impact of the boundary conditions on the DFs is examined. Having seen good agreement between analytical and measured strain data at quarter span (assuming partial restraint) the numerical model is used to predict the DFs at midspan. These are then compared to the DFs specified in DMRB Standard Specification. DFs considered in this study are related to bending moment and DFs for shear are not included within the scope of this study. Stress based DFs were computed using the following equation.

$$DF_i = \frac{\sigma_i}{\sum \sigma_i} = \frac{E_i \varepsilon_i}{\sum E_i \varepsilon_i} = \frac{\varepsilon_i}{\sum \varepsilon_i} \qquad (1)$$

Where:

σ_i = stress at soffit of girder i
E_i = Modulus of Elasticity of concrete
ε_i = Strain measured at soffit girder i

Modulus of elasticity values is assumed to be constant for all girders.

Since it was not possible to install strain sensors at midspan, further analyses were carried out with the bridge FE model loaded with an equivalent truck load at all lanes at midspan to obtain the relevant DF of the deck structure. Truck axle positions were located so that centre of gravity was in line with midspan location and results obtained from the FE model were compared with DFs provided in the Design Manual for Roads and Bridges (DMRB) Standard Specification [9]. DFs for bridge construction with a

concrete deck on precast I-girders are derived from relevant graphs provided in DMRB Standard Specification as 0.495 and 0.472 for internal and external girders, respectively. The DFs calculated from the DMRB Standard Specification depend on the spacing of the girders, span length, skew angle and the number of lanes on the bridge. Fig. 10 illustrates simulated strains obtained for different boundary conditions and corresponding DFs calculated from numerical models. These are compared with calculations using DMRB Standard Specification for 32 tonne truck loaded in each lane. Fig. 11 (a) shows the midspan strain in each of the 12 girders when there are 4 trucks "parked" at midspan, i.e. one truck in each of lanes 1-4. As with quarter span the magnitude of the strain experienced is sensitive to the boundary conditions simulated. Fig 11 (b) shows the corresponding transverse load distribution factors (DFs) for each of the 12 girders (calculated using Eq.1) for three different boundary conditions (hinge-hinge, hinge-roller, and partially fixed). It can be seen in the figure that the hinge-hinge and partially fixed boundary conditions lead to higher DFs than the hinge – roller boundary condition, i.e. greater restraint at the end of the beam leads to less load sharing between adjacent members. The horizontal dashed line in the plot shows the DFs specified by DMRB Standard Specification for an internal girder (for simply supported boundary condition). This value is slightly conservative with respect to the hinge roller boundary condition (which is likely the intention of the code). However, it is actually not conservative if the boundary conditions had changed to hinge – hinge, or partially fixed. The numerical model with partial fixity still includes some errors and such errors, while low, will affect the calculated DF. In Fig. 11(b), any remaining model errors may have caused the DMRB specified DF to appear non-conservative. However, the degree of un-conservativeness is very small, and would likely be offset by the reduction in stress observed in the bottom fibre (due to the restraint).

5.3 Parametric study of boundary conditions vs. midspan moment

The main observation from sections 5.1 and 5.2 is that the structural behaviour of the bridge can be significantly different from that envisaged by the assessment code. To examine this further, in this section a parametric study is carried out to examine how the midspan moment under assessment loading is affected by changes in the boundary conditions. The load to be applied to the beam is determined from the Design Manual for Road and Bridges (DMRB) Standard Specification, then in one simulation the beam is treated as simply supported, in another it is assumed to have the rotational restraints (i.e. longitudinal springs on the top and bottom flanges) observed during the field test, and finally the moment is calculated for a series of intermediate levels of rotation restraint. The analysis presented in this section to calculate a load effect of a girder for different boundary conditions is performed using a simple (1 – D) finite element beam model. Section 5.3.1 gives an overview of the DMRB Standard Specification and section 5.3.2 reports the results of the parametric study.

5.3.1 Overview of loads to be applied during a bridge assessment

Bridges in the UK are assessed to carry the load effects of the Type HA design loading that covers the load effects of vehicles up to 40/44 tonnes. For short to medium span bridges the type HA loading is represented by uniformly distributed load (UDL), derived from equation (2), and applied in conjunction with a knife edge load (KEL) of 120kN [9].

$$W = 336\left(\frac{1}{L}\right)^{0.67} \qquad (2)$$

Where:

W = is the uniformly distributed load in KN per metre length of a lane

L = is span length in metres.

The type HA UDL and KEL loadings specified in DMRB Standard Specification are determined using probabilistic approaches based on the four elements which are a) loading from all the possible vehicles controlled by The Road Vehicle (Authorised Weight (AW)) Regulations 1998 as amended, b) Impact, c) Overloading and d) Lateral bunching.

Loading from AW vehicles is applied to the type HA load model by assuming that all lanes on a bridge structure are fully loaded with particular vehicles. Impact associated with dynamic effects of traffic loading is included only for a single vehicle and a factor of 1.8 is applied to the heaviest axle based on the report published by TRRL [10]. The effect of overloading is estimated based on the surveys carried out by TRRL where static weights of vehicles were monitored at three main road sites and applied in terms of extreme overloading factor which is derived dependent on a span length [11, 12]. Lateral bunching, which is a possibility of having two lines of convoys in a lane, is applied as a factor based on the ratio of standard lane width, 3.65 m, to the maximum width of a vehicle, 2.5 m. Each of these elements described above includes a certain level of conservatism in some form.

Recent data indicates that type HA loading used for design purposes can be relaxed for assessment activities to get less onerous effects, while maintaining the consistent reliability level for the whole network [13]. Besides, probabilistic studies show that impact factor due to dynamic effect of traffic loading, which occurs at high speeds, should not be considered together with lateral bunching. Therefore, DMRB advices a reduction factors such as Adjustment Factor (AF) and Reduction factor (K) to be applied both for UDL and KEL. Hence, Bridge Specific Loading specified by DMRB Standard Specification was calculated by multiplying both UDL and KEL with

Reduction factor and dividing by Adjustment Factor. The Type HA loading was also factored with partial factor (γ_{fL}) to give the 40/44 tonnes Assessment Live Loading and Assessment Load Effect factor (γ_{f3}) to account for any inaccuracies involved in a bridge assessment activity, i.e. inaccuracies involved in calculation models.

5.3.2 Calculating load effects and results of parametric study

Having applied the loads specified in section 5.3.1 to the deck, Assessment Load for a single girder (critical) was obtained by multiplying the load of a single lane by the transverse load distribution factors (DFs) provided in DMRB Standard Specification. Once the load to be applied to an individual girder was known the load effect (midspan bending moment) was calculated using a simple finite element beam model. If simple supports are assumed, there is no need for a finite element model. However, the objective of this section is to examine how midspan moment is affected by varying the level of rotational restraint at the support so a 1-D numerical model is required for this. Work by [14] shows that the longitudinal stiffness of an elastomeric bearing decreases with increasing load. Buckle and Kelly approximated the relationship between axial load and longitudinal stiffness as follows [15];

$$K_{spr} = K^{*}_{spr}\left[1 - \left(\frac{P}{P_{cr}}\right)^{2}\right] \qquad (3)$$

Where:

P = axial load
P_{cr} = critical axial load at particular horizontal displacement
K^{*}_{spr} = longitudinal stiffness of an elastomeric bearing at zero axial load
K_{spr} = longitudinal stiffness of an elastomeric bearing under axial load (P)

Essentially the end restraint if the deck is loaded with HA loading is likely to be

significantly less than the level of end restraint observed when the deck is loaded with a single 32 tonne truck. Therefore, three different spring coefficients were simulated being 100%, 60% and 30% of the spring stiffness obtained from the field testing (with a 32 tonne truck). Table 3 identifies the different loads and factors that were common to all simulations. Table 4 presents the assessment parameters that changed slightly with variation in end restraint, and the bold text in the table shows the bending moment for each case. The italic text in the last row shows the ratio between the midspan moment predicted by the FE model with partial restraint and the simply supported model. In the table, it can be seen that if the end restraint is simulated as being 30% of the full restraint when there was a 32 tonne truck on the bridge this still results in a midspan moment which is 18% less than if the girder is assumed to be simply supported. Admittedly the level of end restraint under Ultimate Limit State (ULS) (DMRB) loading is unknown and in the absence of any other information assuming zero restraint (i.e. assume simply supported) is conservative and appropriate. However, the results in Table 4 show that in a situation where a bridge marginally fails an initial load carrying assessment, some field testing might uncover behaviour (at loads lower than HA loading) that would allow the assessor to revise his structural model (at ULS loading) sufficiently such that bridge would pass the assessment.

6 Summary and Conclusions

A load test was conducted on the North Span of the Exe North Bridge in Exeter, UK where 12 strain transducers were attached to the soffit of the girders at quarter span to record static strains due to a four-axle, 32 tonne truck. Subsequently, 3-D FE model of the bridge was developed and calibrated based on the field test data. The following conclusions result from this study:

- Change in boundary conditions (i.e. degree of translational restraint at the supports) can significantly reduce bending moment effects at midspan in bridge girders.
- Greater restraint at the end of a deck leads to reduced load sharing between girders and as a result, increases transverse load distribution factors (DFs) and hence reduces load carrying capacity of a structure.
- Field testing is an important topic in an effort to dealing with evaluation of aging bridge assets, with a capability to reveal hidden strength reserves.

7 Acknowledgements

This research project has received funding from the European Union's Horizon 2020 research and innovation programme under the Marie Skłodowska – Curie grant agreement No. 642453. The authors would like to acknowledge the Devon County Council, in particular, Mark Colville for facilitating the field test. Additionally, the authors also wish to thank undergraduate student Nick Trump for his assistance during the field test and data analysis.

Tables

Table 1 Summary of the bridge structural characteristics

Total bridge length	59.35m
Number of spans	3
Span lengths	19.85m, 19.61m, 19.85m
Continuity	Simple supported
Skew angle	15 degrees
Deck type	composite I-girders in situ RC deck
Deck width	18.9m
Number of lanes	4
Deck depth	1m
Substructure type	Cantilever type abutment and wall-type pier
Bearing type	Laminated elastomeric bearing

Table 2 Axle weight configuration of the test vehicle

Truck Axles	Axle Weight (kN)
Axle – 1 (Front)	67.2
Axle – 2	67.2
Axle – 3	89.8
Axle – 4 (Rear)	89.8

Table 3 Common parameters used in assessment

Uniformly Distributed Load (kN/m)	Knife Edge Load (kN)	Adjustment Factor	Reduction Factor	Partial Factor (γ_{fL})	Assessment Load Effect factor (γ_{f3})
46	120	1.46	0.78	1.5	1.1

Table 4 Summary of the results for Assessment Live Load calculations

Type HA Load and associated factors	**Simply Supported Model (DMRB)**	**Partially restrained Model (DFs obtained from the field testing)**		
		30% K_{spr}	**60% K_{spr}**	**100% K_{spr}**
Transverse Load Distribution Factor (DF)	0.495	0.512	0.512	0.512
Assessment Live Load - UDL	20.1	20.8	20.8	20.8
Assessment Live Load - KEL	52.4	54.2	54.2	54.2
Assesment Live Load effect (Moment) on critical girder	**1232 kN.m**	**1061 kN.m**	**913 kN.m**	**845 kN.m**
Ratio	*1.0*	*0.82*	*0.74*	*0.69*

Figures

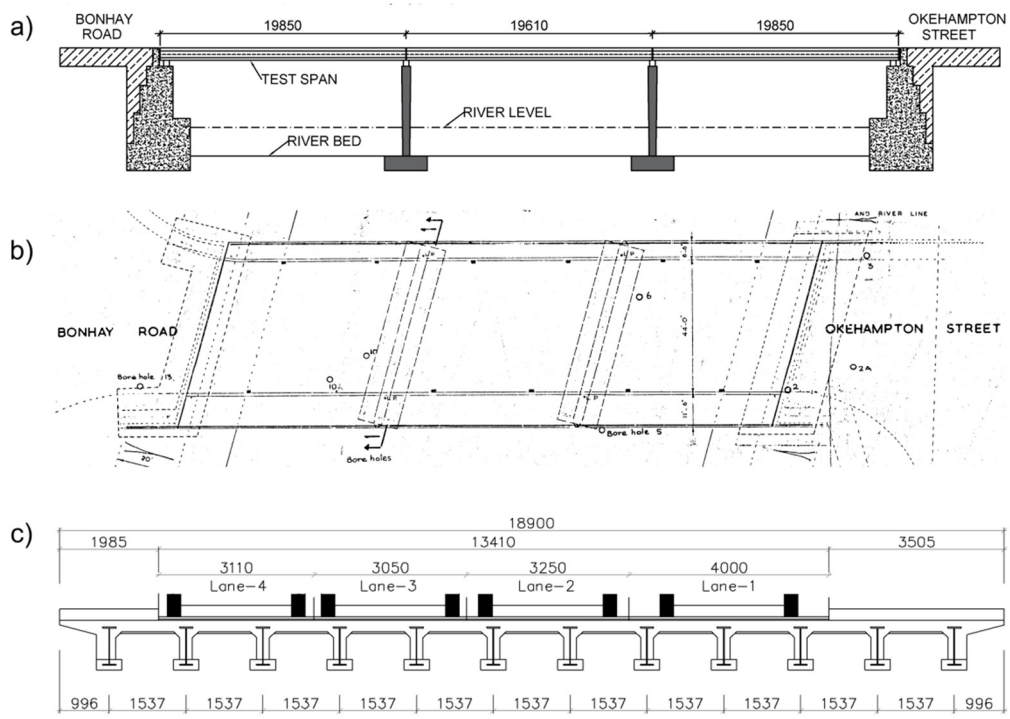

Fig. 1 (a) Bridge elevation. (b) Plan view of Exe North Bridge (c) Cross section of the superstructure

Fig. 2 Exe North Bridge spanning River Exe

Fig. 3 Strain Transducer attached on a girder soffit with an aluminium extension rod

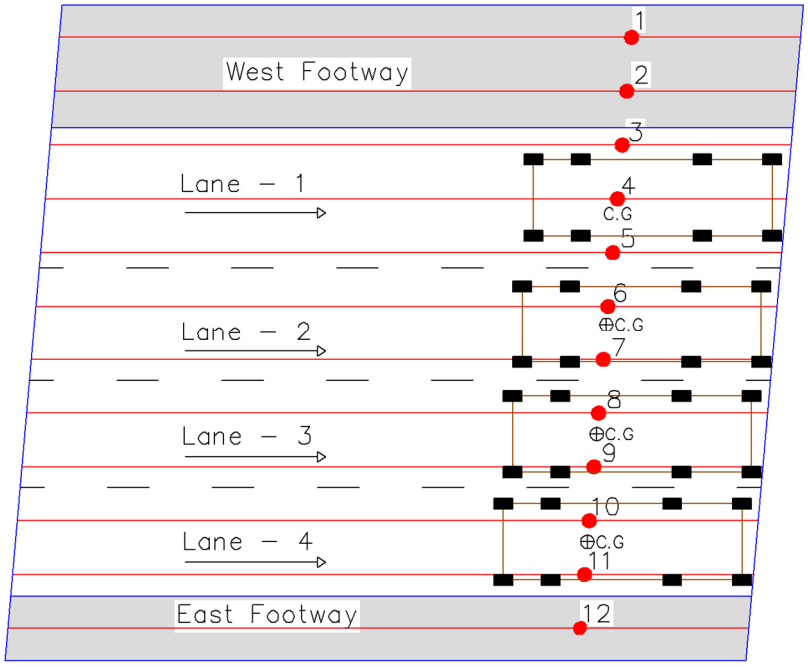

Fig. 4 Sensor and vehicle location layout

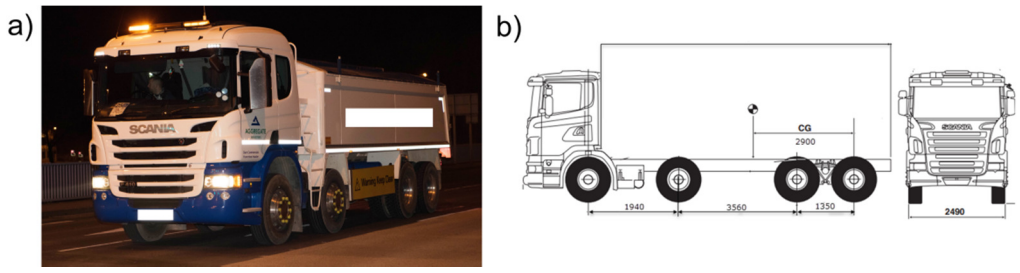

Fig. 5 (a) Test vehicle in the first lane during load testing (b) Axle configuration of the test vehicle

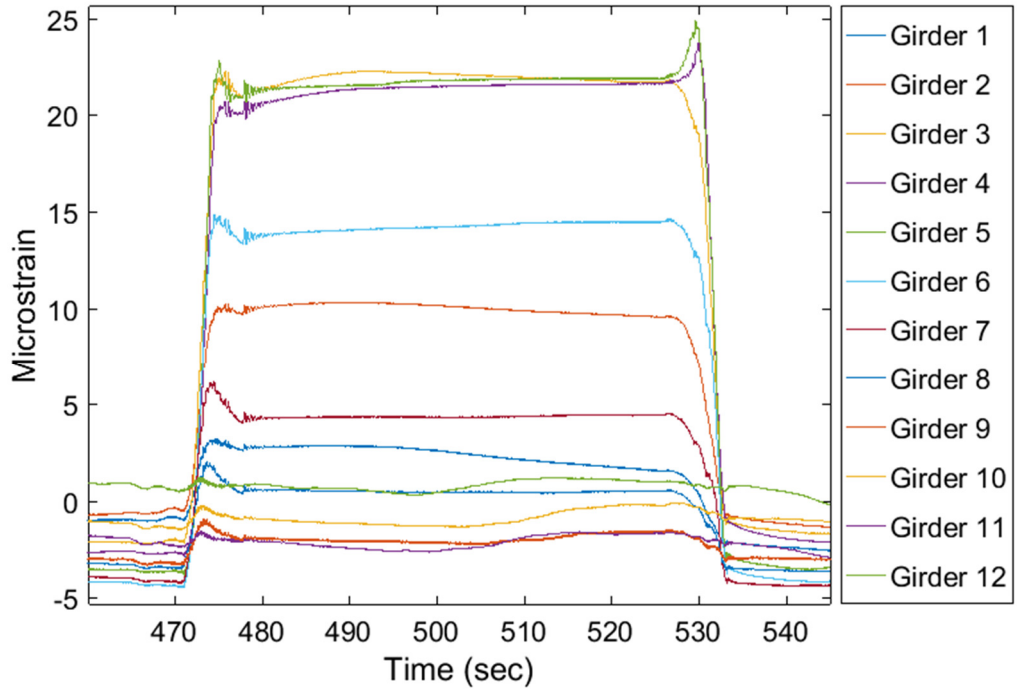

Fig. 6 Typical strain time history graph recorded during the test while vehicle remaining stationary at Lane – 1

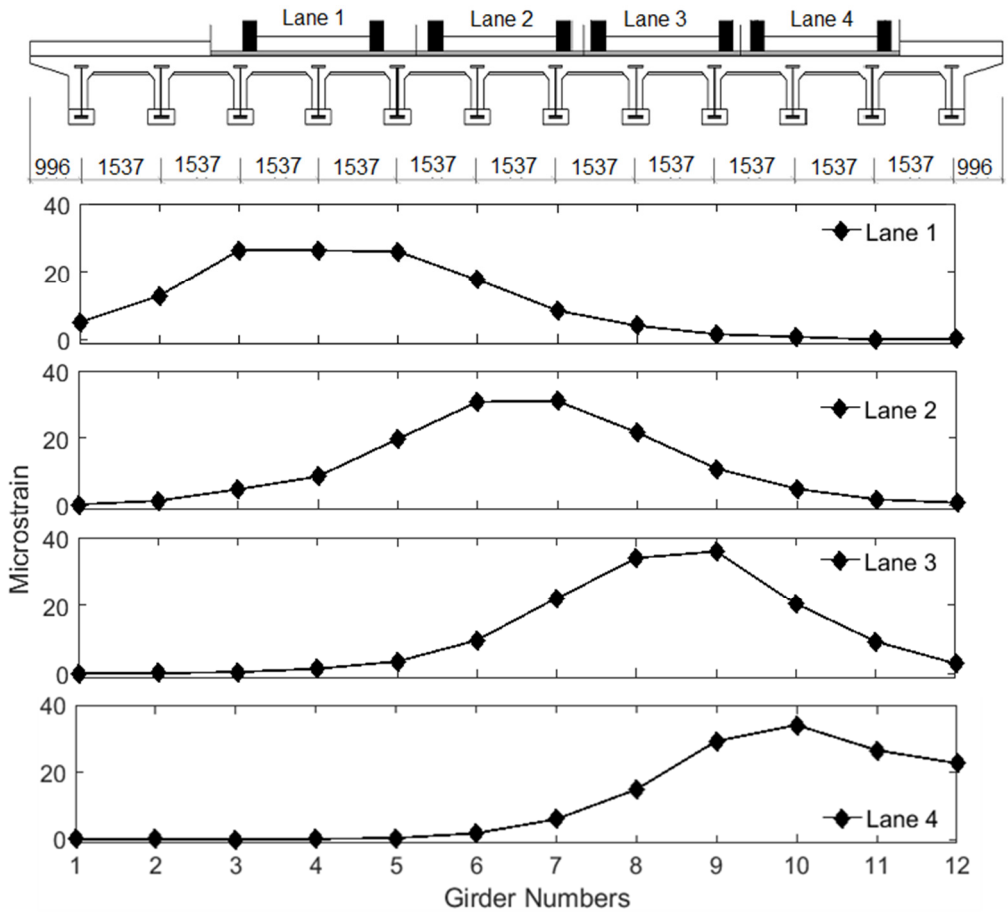

Fig. 7 Strains obtained at the girder soffits during the field test for each lane loading

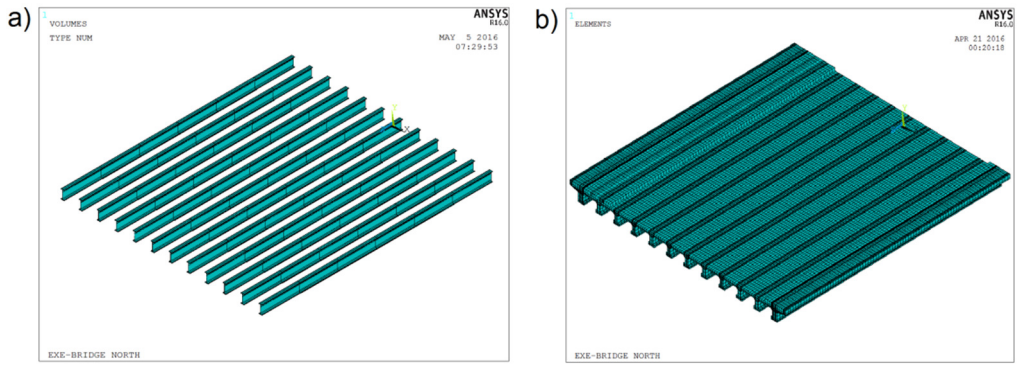

Fig. 8 (a) FE model of steel stringers (b) 3-D FE model of the bridge

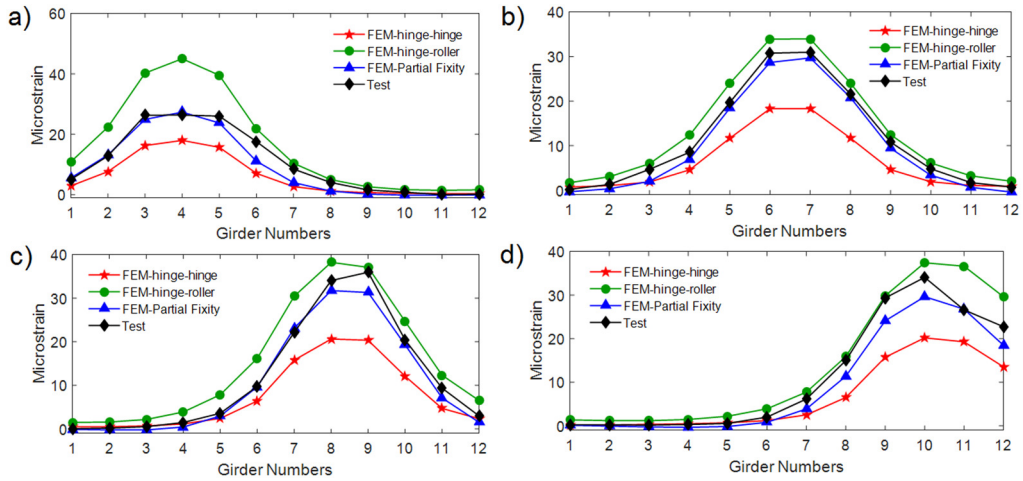

Fig. 9 Strains obtained at the girder soffits during field test and from FE model (a) Lane 1 (b) Lane 2 (c) Lane 3 (d) Lane 4

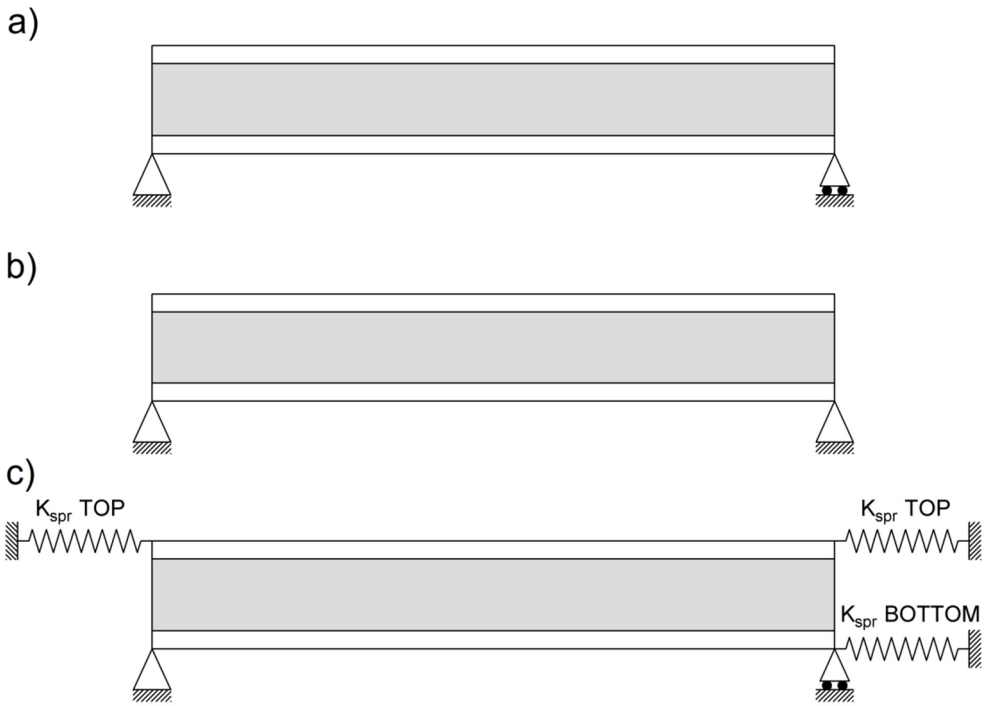

Fig. 10 Three cases of boundary conditions used for finite element analysis. a) hinge – roller b) hinge – hinge c) partially fixed.

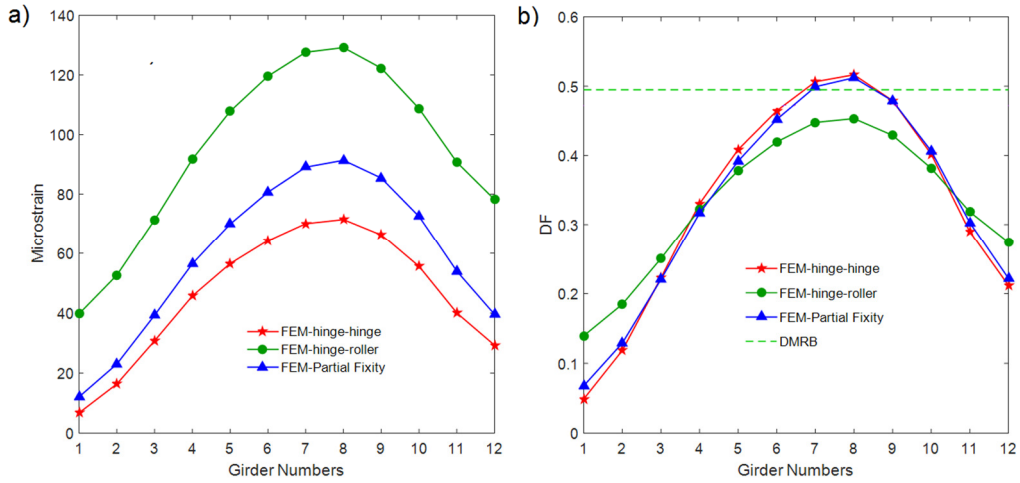

Fig. 11 (a) Strains at midspan under full lane loading (b) DFs at midspan

References

[1] Znidaric A, Pakrashi V, O'Brien E, O'Connor A (2011) A review of road structure data in six European countries. Proceedings of the Institution of Civil Engineers - Urban Design and Planning 164(4):225–232

[2] Das P (1997) Safety of bridges. Telford, London

[3] Bakht B, Jaeger L (1990) Bridge testing—a surprise every time. J Struct Eng 116(5):1370–1383

[4] McConnell J, Chajes M, Michaud K (2015) Field testing of a decommissioned skewed steel I–Girder bridge: analysis of system effects. J Struct Eng 141(1):D4014010

[5] Puurula A, Enochsson O, Sas G, Blanksvard T, Ohlsson U, Bernspang L, Taljsten B, Carolin A, Paulsson B, Elfgren L (2015) Assessment of the strengthening of an RC railway bridge with CFRP utilizing a full-scale failure test and finite-element analysis. J Struct Eng 141(1):D4014008

[6] ANSYS (2015) Academic Research, Release 16.0, ANSYS Mechanical User's Guide. Ansys Inc

[7] Barr P, Eberhard M, Stanton J (2001) Live-load distribution factors in prestressed concrete girder bridges. J Bridge Eng 6(5):298–306

[8] Bishara A, Liu M, El-Ali N (1993) Wheel load distribution on simply supported skew I-beam composite bridges. J Struct Eng 119(2):399–419

[9] Highways Agency (2000) Design manual for roads and bridges. Stationery Office, London

[10] Page J (1976) Report 722: Dynamic wheel load measurements on motorway bridges. Transport and Road Research Laboratory

[11] Glover MH (1983) Supplementary Report 770: Results from the Hull axle weight survey. Transport and Road Research Laboratory

[12] Glover MH, Shane BA (1983) Supplementary Report 787: Results from axle weight surveys at Lichfield and Barham. Transport and Road Research Laboratory

[13] Dawe P (2003) Research perspectives. Thomas Telford, London

[14] Buckle I, Nagarajaiah S, Ferrell K (2002) Stability of elastomeric isolation bearings: experimental study. J Struct Eng 128(1):3–11